# POLITECNICO
## MILANO 1863

# Reverse Engineering of Juno Mission
## Final report

Course of Space Systems Engineering & Operations
Academic Year 2023-2024

# Group 5

| | | |
|---|---|---|
| Alex Cristian Turcu | alexcristian.turcu@mail.polimi.it | 10711624 |
| Chiara Poli | chiara3.poli@mail.polimi.it | 10731504 |
| Daniele Paternoster | daniele.paternoster@mail.polimi.it | 10836125 |
| Marcello Pareschi | marcello.pareschi@mail.polimi.it | 10723712 |
| Paolo Vanelli | paolo.vanelli@mail.polimi.it | 10730510 |
| Riccardo Vidari | riccardo.vidari@mail.polimi.it | 10711828 |

# Contents

# Homework 1

## Notation

| | |
|---|---|
| **MAG** | Magnetometer |
| **HGA** | High Gain Antenna |
| **ΔV** | Velocity budget |
| **DSN** | Deep Space Network |
| **LEOP** | Launch and early orbit phase |
| **SECO** | Second engine cut off |
| **L+** | Time after launch |
| **PJ** | Perijove number |
| **MWR** | Microwave Radiometer |

| | |
|---|---|
| **JEDI** | Jupiter Energetic-particle Detector Instrument |
| **JADE** | Jovian Auroral Distribution Experiment |
| **UVS** | Ultraviolet Spectrograph |
| **JIRAM** | Juno Infra-Red Auroral Mapper |
| **EGA** | Earth Gravity Assist |
| **JOI** | Jupiter Orbit Insertion |
| **DSM** | Deep Space Manoeuvre |
| **PRM** | Period Reduction Maneuver |
| **GSO** | Gravity Science Orbit |

## 1.1 Introduction

Juno is a NASA spacecraft orbiting Jupiter. Built by Lockheed Martin and operated by NASA, it was launched by an Atlas V551 on the $5^{th}$ of August 2011. After 5 years, during which many maneuvers occurred, including an Earth flyby, Juno entered a polar orbit around Jupiter and started its observation, which lasts to this day. Its aim is to study the planet to understand its composition and evolution, analyzing its gravitational and magnetic fields and its atmosphere dynamics. The mission should have ended in 2017, but it is still ongoing[1] and it will end with a de-orbit that will destroy the spacecraft into the planet's atmosphere to avoid contaminating the environment.

## 1.2 High level goals

Through an analysis of the mission and payload, the main goals of the mission can be highlighted.

1. **How did Jupiter form and influence the solar system?**[2][3]
   Since Jupiter is the biggest planet of the solar system, it has influenced the formation of all other planets. Its composition has remained unchanged ever since, making it like a time capsule: understanding how and where it formed could give knowledge on Earth and the whole solar system's origin, evolution and characteristics.

2. **What's Jupiter's deep structure?**[3][4]
   One important aspect of the mission is the analysis of Jupiter's deep structure through the measurement of radiations, magnetic and gravitational fields. This allows to comprehend whether or not the planet has a solid nucleus, if so how large it is, and to analyze the supposed layer of metallic hydrogen, compressed so much that it loses its electrons creating a conducting layer. Moreover, Juno will possibly reveal if Jupiter is rotating as a solid body or if the rotating interior is made up of concentric cylinders.

3. **What's the structure of Jupiter's atmosphere?**[3][5]
   One of the mission's goals is to study the composition and dynamics of Jupiter's atmosphere, composed by stripes and dots made of different gasses and vapors, including water, whose percentage has to be defined. A significant aspect of the analysis is the great red spot, a swirling mass of gas bigger than Earth, which resembles a hurricane but is very different in the way it works. The movement of stripes and dots is dictated by the weather, characterized by lighting an thunderstorms, which are observed by Juno.

4. **What do auroras look like and what are the physical processes generating them?**[3][5]
   Juno's orbit is designed to be polar, to allow the observation of Jupiter's poles and the analysis of its auroras, representative of the interaction between charged particles and the atmosphere. Studying this phenomenon allows a better understanding of the atmospheric composition and the magnetic field's structure and extension.

5. **What do the poles look like?**[3]
   One of Juno's side goals is the observation of Jupiter's poles, which had never been possible before because of the absence of a polar orbiting spacecraft. This also increments the public's involvement in the mission.

## 1.3 Mission drivers

Being Juno an interplanetary mission starting from a distance of around 1 AU, with a final nominal distance from the Sun of 5.2 AU, and operating in an highly radiation intense environment, the following drivers have been identified:

1. **Using proven technologies**[6]
   The total program is financed with 1.1 Billion $ for 74 months from the launch date and includes development of the spacecraft, science instruments, launch services, mission operations, science processing and relay support. The simplicity and the need of proven technologies was thus fundamental. The spacecraft is mainly maintained stable during the manuevers thanks to its spin, raised to 5 RPM from 2, nominal condition during science operations, reducing the need of active stabilization methods.

2. **Providing enough electricity during the duration of the mission**[3][6][7][8][9]
   The journey of Juno is long and passes through different regions of the solar system. Solar panels were chosen to provide electric energy across the mission over a nuclear source, since it has been decided that it was better to advance technology of solar cells rather than developing a new reactor. It is the first spacecraft to operate with solar panels at such distance from the Sun. The system needed is thus oversized at 1 AU: the solar radiation on Jupiter is in fact up to 96% lower than on Earth. Furthermore the operations are scheduled to begin around 5 years into the mission, so degradation of the solar cells must be taken into account. The final design consists in 11 solar panels, eight are 9 by 2.65 m each, meanwhile the inner three are only 2 m wide, resulting in a surface of about 60 $m^2$ and granting a maximum power of 14 kW around Earth and up to 500 W around Jupiter. The solar panels are mounted in three arrays on the side of hexagonal body of the spacecraft at 120° one by the other, three arrays are composed by 4 panels, one by 3. This configuration is needed to mount the MAG faraway from the electronics and store everything correctly inside the fairing. Before separation from the upper stage, the spacecraft is spinning at around 1.4 RPM and the deployment of the solar arrays slows it down to 1 RPM. Moreover, since the fly-by around Earth is done to gain $\Delta V$, the spacecraft will be in an eclipse for around 20

minutes: attention must be paid to size the battery. Two lithium-ions battery of 55 Ah each are present to make sure power is always provided. The nominal polar orbit around Jupiter allows Sun pointing during the majority of nominal Science Operation phase.

3. **Shielding the instruments from the harsh environment of Jupiter**[1][2][10][11]
   To accomplish its goals, Juno will need to cross the Jupiter radiation belts: a heavy shielding structure is needed. The magnetosphere represents a great challenge for Juno: the value of the magnetic field measured at its perijove is 776 $\mu$T, 50% higher than expected. The main issue with Juno is represented by the ionizing particles present in the belt around Jupiter: with measured value up to of tens and hundreds of MeV ions located between 2 and 4 $R_J$, order of GeV were expected under 2 $R_J$, where Juno should pass through to reach a lower altitude, thanks to its highly elliptical orbit, where radiations are lower, to perform science. The vault in which all the electronics is preserved is cubed shaped and it is made of 1 cm thick titanium alloy, 144 kg in total. The top deck of Juno is planned to receive a radiation dose of 22 Mrad. Moreover, star trackers are also heavily shielded.

4. **Maintaining communication during the journey and the science operations**[6]
   The attitude of the spacecraft is defined in a way to point Earth during most of the cruise and science operations. This configuration, given the distance from the Sun and the Earth, grants also a sufficient inclinations of the solar panels with respect to the Sun to provide enough electric power. The ground equipment used by Juno is NASA's DSN.

## 1.4 Functional analysis

Functional analysis is performed in order to identify the functionalities that the spacecraft must perform during the mission. The identified functionalities are schematized in Figure 1.1.



Figure 1.1: Functional analysis for Juno mission

## 1.5 Main mission phases

The Juno mission was divided into five phases: LEOP, Cruise, Jupiter approach and insertion, Science Operations and De-orbit.

1. **LEOP**
Following the launch from Cape Canaveral, the spacecraft entered a low Earth parking orbit.[6] Afterwards Juno was injected in an interplanetary trajectory and was separated from its upper stage after SECO-2 at time L+54 min. The solar panels deployment was performed about five minutes after the spacecraft separation, and it took approximately five minutes.

2. **Cruise**
The cruise had a duration of about five years, during which two deep space manoeuvres, multiple minor corrections and an Earth fly-by were performed. All manoeuvres will be better described in section 1.8. This phase also included instruments testing and verification, to ensure they were functioning properly and ready for the usage during the mission.

3. **Jupiter approach and insertion**
This phase began four days before the start of orbit insertion manoeuvre and ended one hour after the start of the orbit insertion manoeuvre. The latter occurred at closest approach to Jupiter and slowed the spacecraft down enough to let it be captured by Jupiter in a 53-days period orbit. The Jupiter orbit insertion burn was performed by the Leros 1-b main engine, and it lasted 30 minutes. After the burn, the spacecraft was in a polar orbit around Jupiter. The 53-days orbit provided substantial propellant savings with respect to the direct insertion in the operational orbit.

4. **Science operations**
The Juno polar and highly eccentric orbit was designed to facilitate the close-in measurements and to minimize the time spent in the Jupiter radiation belts. During this phase all the science operations, in different attitudes, are being performed.

5. **De-orbit**
The de-orbit phase will occur during the final orbit of the mission. The latter was designed to satisfy NASA's planetary protection requirements and ensure that Juno doesn't impact any of Jupiter's moons. A de-orbit burn will be performed, placing the spacecraft on a trajectory towards Jupiter inner and denser layer of the atmosphere where it will burn up.

## 1.6 ConOps

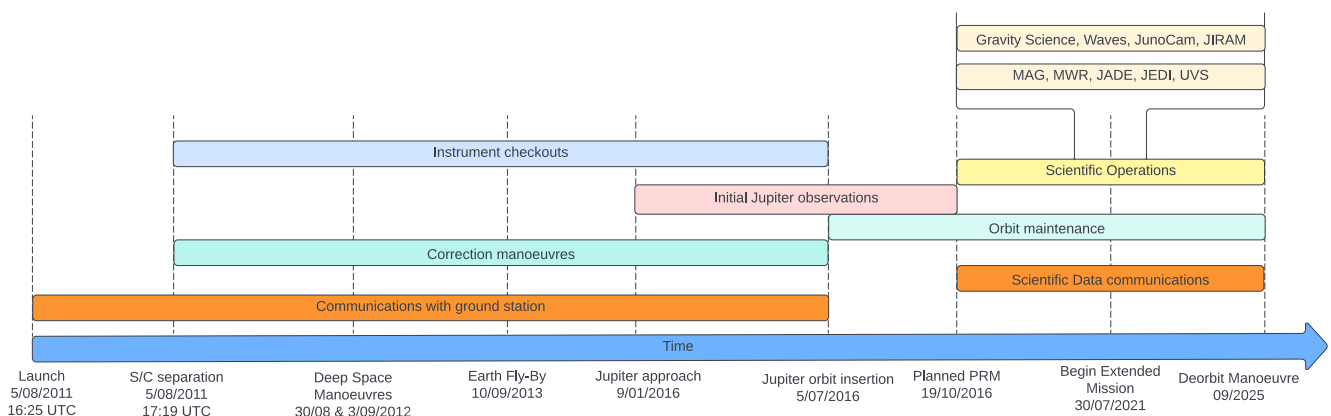The mission's Conceptual Operations are summarized in Figure 1.2.



Figure 1.2: Conceptual Operations, time not in scale[2][6][12][13]

## 1.7   Payload analysis

### 1.7.1   Instruments overview

As previously described in section 1.2 the mission scientific goals are quite numerous and diverse. Thus, to achieve all of them, the payload consists of several instruments, nine to be precise, covering a wide spectrum of experimentation. In its entirety the payload has a mass of around 174 kg and consumes approximately 125 W of power excluding the Gravity science experiment.[7] Here we have a brief overview of all the singular instruments where, unless otherwise specified, only the sensors are mounted on the exterior of the spacecraft, while all the relevant electronics are located inside the radiation vault.

- **Magnetometer (MAG):** As the name implies its objective is to accurately measure Jupiter's magnetic field, achieved by employing two flux-gate magnetometers, a scalar helium magnetometer and two star cameras. All the sensors are mounted on the magnetometer boom, located at the end of one of the solar array wings to reduce the interference from the spacecraft itself. Even then the presence of two magnetometers allows to subtract this contribution from the measurement.

- **Microwave Radiometer (MWR):** It consists of six antennas which measure six different frequencies (600 MHz, 1.2 GHz, 2.4 GHz, 4.8 GHz, 9.6 GHz and 22 GHz) in order to investigate the Jovian atmosphere below the visible external layer. A key objective of this analysis is also the determination of the abundance of water inside the planet. The antennas are mounted on two sides of the hexagonal prism that constitutes the main body of the spacecraft, relying on its spin to survey Jupiter.

- **Gravity science:** It's quite a unique instrument as it's composed both by a space and a ground elements, which mainly consists with the telecommunication systems of both the spacecraft and ground stations. This is because this experiment is based on measuring the doppler shift in the returning signal from Juno which, allows to characterize Jupiter's gravitational field. Thus the instrument can't really be separated from the telecommunication hardware, which is the reason why its weight and power requirement were omitted in the previously shown totals.

- **Jupiter Energetic-particle Detector Instrument (JEDI):** It detects high energy electrons and ions present in the Jovian magnetosphere, which are discriminated by composition. Each sensor is characterized by six electron and six ion viewing directions that together cover a $160° \times 12°$ field of view. In total three sensors are present on Juno, two arranged to obtain an almost compete $360°$ view perpendicular to the spacecraft spin axis, while the third one is instead aligned with it to achieve a full scan of the sky over one spin period. As the JEDI sensors are self-contained units no electronic hardware is present within the radiation vault.

- **Jovian Auroral Distribution Experiment (JADE):** It detects low energy electrons and ions with the same goal of characterizing the magnetosphere as JEDI. The instrument comprises of three identical electron energy per charge analyzers (JADE-E) and a single ion mass spectrometer (JADE-I). The electron sensors are located on the three sides of the spacecraft that do not house the solar arrays pointing outwards, to again obtain a complete view normal to the spin axis. The spectrometer field of view, instead, contains the spin axis and like the third JEDI sensor it scans all the sky over a full rotation.

- **Ultraviolet Spectrograph (UVS):** This instrument images and measures the spectrum of the Jovian aurora in order to understand its morphology and source. The chosen ultraviolet range of $68 \div 210$ nm covers all of the most important UV emissions form the aurora, mainly the H Lyman series and longer wavelengths from hydrocarbons. The sensor is mounted on the side of Juno, relying once more on the spinning of the spacecraft to achieve a full sweep of the planet.

- **Radio and Plasma Waves (Waves):** Its objective is to study both components of the electromagnetic field generated by plasma and radio waves inside the polar regions of Jupiter's magnetosphere to understand its interaction with the atmosphere and magnetic field. To detect the electric component a V-shaped dipole antenna is used, while for the magnetic component a much smaller magnetic search coil is employed. Both sensors cover a vast range of frequencies, namely from 50 Hz up to 40 MHz.

- **Visible-spectrum Camera (JunoCam):** It's designed to provide highly detailed color images of Jupiter to help and support public engagement of the mission without any real scientific purpose. The instrument is thus only comprised of the camera itself, mounted on the side of the spacecraft, and all the necessary electronics which, given the less critical objective and relaxed radiation tolerance requirements, aren't housed in the radiation vault.

- **Juno Infra-Red Auroral Mapper (JIRAM):** It's an infrared imager and spectrometer that studies the Jovian atmosphere in the $2 \div 5$ $\mu$m range complementing both the atmospheric and magnetospheric experiments. This instrument is also completely housed outside of the radiation vault since it is a late addition after mission selection, reason for both the relaxed radiation requirements and less than ideal positioning of the sensor on the aft deck of the spacecraft.

All the instruments and their positions can be seen in Figure 1.3.



Figure 1.3: Positioning of the instruments on the spacecraft

## 1.7.2   Payload and Goals correlation

There is a notable overlap in the main objectives of the payload instruments, both in the sense that multiple ones collaborate towards a single scientific goal, but also in the sense that a single instrument can address multiple goals. All of these relations are exemplified in Table 1.1.

| Guiding questions | Science objectives | Measurements objectives |
|---|---|---|
| How did Jupiter form and influence the solar system? | Determine Jupiter's inner composition | Composition analysis: MWR |
| What's Jupiter's deep structure? | Analyze gravitational and magnetic field, measure water abundance in the planet | Gravitational field analysis: Gravity science<br>Magnetic field analysis: MAG<br>Water abundance measurements: MWR |
| What's the structure of Jupiter's atmosphere? | Analyze atmospheric composition and dynamics | Atmospheric composition determination: MWR<br>Atmospheric dynamics study: JIRAM |
| What do auroras look like and what are the physical processes generating them? | Image auroras, study interactions between atmosphere and magnetic field, characterize the magnetosphere in the polar regions | Imaging auroras: UVS, JIRAM<br>Atmosphere-magnetic field interaction: JIRAM<br>Characterize the magnetosphere: Waves, JADE, JEDI |

Table 1.1: Mission goals and instrument objectives correlation

It can be noted that the JunoCam instrument doesn't appear in the table since it's not part of the scientific goals of the mission, as previously mentioned in its description.

### 1.7.3 Payload and Phases/ConOps correlation

Another high-level correlation can be highlighted between the mission phases/ConOps and the activities of the payload as shown in Table 1.2.[6]

| Mission phases | Payload activities |
|---|---|
| LEOP | Mag boom is deployed together with solar arrays |
| Cruise | Instruments checks are performed regularly and the high gain antenna (used for Gravity science) is calibrated and aligned |
| Jupiter approach and insertion | Final instruments checks are carried out together with some initial scientific observations of Jupiter |
| Science operations | Complete nominal operation of the payload with observations divided between Gravity science passes (Earth pointing) and MWR passes (Nadir pointing) |
| De-orbit | No planned payload operations |

Table 1.2: Mission phases/ConOps and Payload activities correlation

## 1.8 Mission analysis

### 1.8.1 Launch and cruise

The spacecraft was launched into orbit with an Atlas V 551 Rocket from Cape Canaveral. The actual launch date belonged to a 21-day time window limited by a number of events and their timings such as the Deep Space Maneuvers, the Earth Flyby, the Jupiter Insertion and the science orbits. The adopted transfer strategy allowed for significant reduction in $\Delta V$ with respect to a direct transfer between Earth and Jupiter.

Following the launch, after booster separation, Juno was put in a low Earth parking orbit thanks to a first burn of the Centaur upper stage. Afterwards, at time L+645 s, via a second burn given by the same stage, Juno entered an heliocentric trajectory. Solar arrays were deployed and initial checks on the instruments were performed at this time. This procedure is fundamental in order to provide enough electrical power to the spacecraft to perform initial check on its health. The specific trajectory followed by Juno is called "2 + dV-EGA", which means that the spacecraft will perform an Earth gravity assist at around two years after launch. During the initial cruise various correction maneuvers were performed: the main ones being the two DSMs needed to place Juno on the correct path to achieve the planned fly-by. DSMs were performed near the apocentre, located farther away from the Sun than Mars' orbit, causing the spacecraft to pass as close as 0.88 AU before approaching Earth. During the approach to perform the fly-by, attitude corrections were performed to protect the spacecraft by the incoming radiation from the Sun. The fly-by around Earth occurred on the $10^{th}$ of September 2013 and puts the spacecraft on its final trajectory to Jupiter. Particularly, the fly-by gave the spacecraft 7.3 km/s, avoiding a fire-up of the Leros 1-b main engine of Juno. A last correction maneuver was performed to refine Juno's trajectory.[4][6][9][14][15]
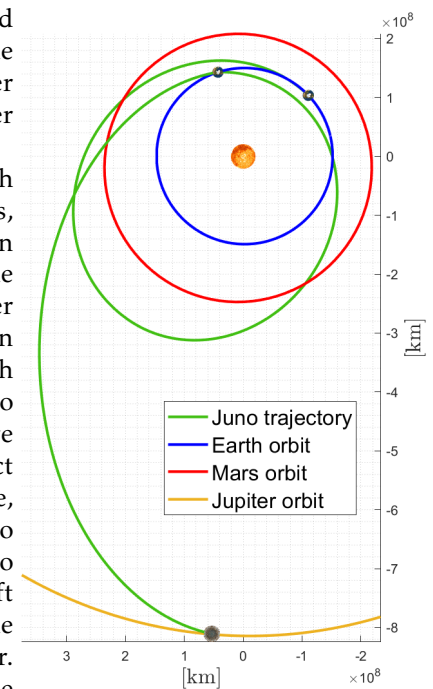


Figure 1.4: Juno's trajectory from ecliptic north pole

### 1.8.2 Jupiter approach and insertion

After the flyby, Juno spent 791 days on its last interplanetary leg in which no significant manuevers nor scientific operations were conducted. Jupiter approach lasted a further 178 days, during which calibration, validation of the on board instruments and telecommunications checks were accomplished. Initial science observations of Jupiter's distant environment were also performed.

JOI burn was made at the closest approach to Jupiter: this moment is called PJ-0, indicating the first passage at the perijove of Juno. The targeted point for this maneuver is at an altitude of 4200 km, calculated above the 1-bar level of Jupiter. The spacecraft is left on a highly elliptical 53-days period around Jupiter with and inclination of 90° (±10°). Additional clean-up manuevers were planned to correct the trajectory. The attitude during JOI phase, as the

spacecraft was slowing down, was such that the HGA was not pointing Earth, constraining communications to low tones, only meant to send information about the completion or failure of the events. After 50 hours from PJ0 all instruments were successfully powered up and started to perform nominal science operations.

### 1.8.3 Science operations and extended mission

The nominal science orbit, with a period of 14-days, had to be achieved via a PRM at PJ-02. This orbit had been chosen for many reasons:

- it allowed to avoid Jupiter's strongest radiation belts
- enabled near Sun pointing to generate enough electrical power and granted Earth communications via HGA
- it provided the closest possible approach of the instruments to Jupiter's clouds
- it allowed, thanks to Jupiter's oblateness, to scan the whole planet with only 32 orbits obtaining a resolution of 11.25°.

During science operations, two types of orbits should have been performed, differing in terms of spacecraft orientation: MWR passes, which required nadir pointing of Juno's spin plane in order to let the radiometers scan directly the planet, and GSOs, designed to align HGA with Earth.

However, due to a malfunctioning of an helium tank valve, Juno entered Safe Mode for 13.5 hours and PRW was discarded. This change showed the robustness of the designed capture orbit. It was in fact possible to conduct science operations on this longer path with only minor changes: the disposal of the spacecraft had to be moved from 2017 to 2021 to allow the completion of the 35 orbits. Moreover, the 53-days orbit required a slight plane change (from 90° to 105°) between PJ-22 and PJ-23 to avoid a solar eclipse since the batteries are only suited for the 19 minutes eclipse during the Earth fly-by.

The so conducted mission was scheduled to end on July 2021 but the conditions of the spacecraft and the remaining fuel on board allowed to extend the mission by other 42 orbits for 5 more years of mission. During the nominal phases, the PJ had been shifted northwards, so during the extended phase a series of close passes of Jupiter's north polar cyclones occurred. Furthermore, flybys of Ganymede, Io and Europa are performed in addition to an analysis of the faint rings of the observed planet.[1]
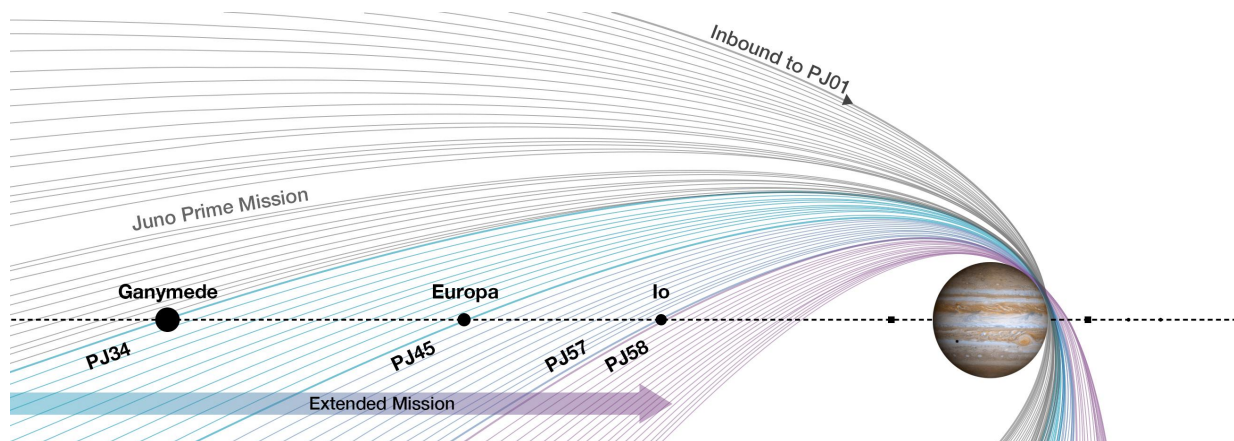


Figure 1.5: Orbits around Jupiter

### 1.8.4 Mission disposal

Under the planetary protection requirements, Juno is designed to de-orbit itself after the extended mission succeeds. The dose of radiations absorbed during the lifetime of the spacecraft won't allow for safe operations. The de-orbit manuever is supposed to begin with an apocentre burn, slowing down Juno by 75 m/s, enough to lower its perijove in the atmosphere of Jupiter. The dense gas layers will cause the spacecraft to disintegrate.

De-orbiting the spacecraft, now planned in 2025, will eliminate the possibility of contamination of Jupiter and its Moons' environment, especially to avoid unreliable results from the planned ESA Juice mission, expected to enter Jupiter's orbit in 2031.[12][13]

# Bibliography

[1]  Jet Propulsion Laboratory. *Juno Mission to Jupiter*. Site: `https://www.nasa.gov/`. 2022.

[2]  Richard Grammier. *Overview of the Juno Mission to Jupiter*. Site: `https://www.jpl.nasa.gov/missions/juno`. 2006.

[3]  Various. *Mission Juno - Great documentary on Jupiter and NASA's Juno probe*. Website. Site: `https://www.youtube.com/watch?v=ka60ERznXh4`. 2013.

[4]  Richard Grammier. "An overview of the Juno mission Jupiter". In: (2006).

[5]  S.J. Bolton J. Lunine D. Stevenson J.E.P. Connerney S. Levin T.C. Owen F. Bagenal D. Gautier A.P. Ingersoll G.S. Orton T. Guillot W. Hubbard. J. Bloxham A. Coradini S.K. Stephen P. Mokashi R. Thorne R. Thorpe. "The Juno mission". In: (2015).

[6]  *Advanced Global Optimisation Tools for Mission Analysis and Design*. NASA press kit. Site: `https://www.jpl.nasa.gov/news/press_kits/JunoLaunch.pdf`. 2011.

[7]  Chuck E. Rasbach Randy Dodge Mark A. Boyles. "Key and Driving Requirements for the Juno Payload Suite of Instruments". In: (2012).

[8]  Stephen F Dawson Paul Stella William McAlpine Brian Smith. *Juno Photovoltaic Power at Jupiter*. Site: `https://ntrs.nasa.gov/citations/20130010565`. 2012.

[9]  Various. *Spacecraft Information*. Website. Site: `https://spaceflight101.com/juno/spacecraft-information/`. 2024.

[10]  Installing Juno's radiation vault. *Radiation vault characteristics*. Website. Site: `https://www.nasa.gov/image-article/installing-junos-radiation-vault/`. 2024.

[11]  Connerney et al. *A New Model of Jupiter's Magnetic Field from Juno'sFirst Nine Orbits*. Journal of Geophysical Research: Planet. Site: `https://agupubs.onlinelibrary.wiley.com/doi/10.1002/2018GL077312`. 2018.

[12]  NASA Jet Propulsion Laboratory. *NASA online press kit*. Website. Site: `https://www.jpl.nasa.gov/news/press_kits/juno/`. 2024.

[13]  NASA Jet Propulsion Laboratory. *NASA's Juno Mission Expands Into the Future*. Website. Site: `https://www.jpl.nasa.gov/news/nasas-juno-mission-expands-into-the-future`. 2024.

[14]  Various. *Juno Mission and Trajectory Design*. Website. Site: `https://spaceflight101.com/juno/juno-mission-trajectory-design/`. 2024.

[15]  NASA Horizons. *Ephemerides Data*. Website. Site: `https://ssd.jpl.nasa.gov/horizons/`. 2024.

# Homework 2

## Notation

| | | | |
|---|---|---|---|
| **ME** | Main Engine | $e_{cap}$ | Eccentricity of capture orbit [-] |
| **RCS** | Reaction Control System | **NTO** | Nitrogen Tetroxide |
| **DSM** | Deep Space Manoeuvre | **O/F** | Oxidizer to Fuel ratio |
| **DSN** | Deep Space Network | $M_{dry}$ | Total dry mass of satellite [kg] |
| **OTM** | Orbit Trim Manoeuvre | $M_{launch}$ | Total mass of satellite at launch [kg] |
| **TCM** | Trajectory Correction Manoeuvre | $M$ | Total mass of satellite [kg] |
| **SK** | Station Keeping | $M_p$ | Total mass of propellants [kg] |
| **PRM** | Period Reduction Manoeuvre | $M_f$ | Total mass of fuel [kg] |
| **JOI** | Jupiter Orbit Insertion | $M_{ox}$ | Total mass of oxidizer [kg] |
| **REM** | Rocket Engine Module | $M_{He}$ | Total mass of helium [kg] |
| **MEF** | Main Engine Flush | $V_{He}$ | Total volume of helium [m$^3$] |
| **TRL** | Technology Readiness Level | $I_s$ | Specific impulse [s] |
| **RW** | Reaction Wheel | $g_0$ | Standard gravitational acceleration [m/s$^2$] |
| **COM** | Centre Of Mass | $r_{tank}$ | Radius of spherical propellants tanks [m] |
| **MAG** | Magnetometer | $p_{tank}$ | Pressure of propellants tanks [Pa] |
| **PC** | Plane Change | $T_{tank}$ | Temperature of propellants tanks [K] |
| **ELA** | Earth Look Angle | $t_{tank}$ | Thickness of propellants tanks [m] |
| **EGA** | Earth Gravity Assist | $V_{tank}$ | Volume of one empty propellants tank [m$^3$] |
| **FB** | Fly-by | $M_{tank}$ | Mass of one empty propellants tank [kg] |
| **INJ$_J$** | Jupiter injection | $r_{tank,He}$ | Radius of cylindrical helium tanks [m] |
| **ESC$_E$** | Earth escape | $h_{tank,He}$ | Height of cylindrical helium tanks [m] |
| **TLGA** | Toroidal Low Gain Antenna | $t_{tank,He}$ | Thickness of helium tanks [m] |
| **HGA** | High Gain Antenna | $M_{tank,He}$ | Mass of one empty helium tank [kg] |
| **SEP** | Sun-Earth-Probe | $R_{He}$ | Specific gas constant for helium [J/kg·K] |
| **PED** | Propellant Expulsion Device | $\gamma_{He}$ | Adiabatic index for helium [-] |
| $\tau$ | Burn time [s] | **Ti6Al4V** | Titanium alloy |
| $\Delta V$ | Velocity change [m/s] | **Al7075** | Aluminum alloy |
| $v_\infty$ | Asymptotic velocity [m/s] | $\rho$ | Density of the material [kg/m$^3$] |
| $\mu_J$ | Jupiter planetary constant [km$^3$/s$^2$] | $\sigma$ | Tensile yield strength of the material [Pa] |
| $r_p$ | Radius of pericentre [km] | | |

## 2.1 Mission analysis and $\Delta V$ budget

### 2.1.1 Rationale of the mission analysis

The mission analysis previously described could be split into two macro-phases:

- from launch to the interplanetary transfer, including DSMs and the Earth fly-by;
- planetary phase around Jupiter.

The main objectives of the mission analysis were to keep the overall launch energy $C_3$ and deterministic $\Delta V$ as low as possible, compliant with the constraints imposed by the navigation and spacecraft operational requirements. Regarding the interplanetary transfer, two main options were available, both including an EGA. The first option, named as "$2 - dV\,EGA$", contemplated a launch window time frame in October-November 2011. However, the latter was discarded since the approach angle at Jupiter would have resulted in a latitude farther away from the equator. This would have brought to higher radiation levels, hence a reduced time available for the science operations[1]. The second option, named as "$2 + dV\,EGA$", contemplated a launch window time frame in August 2011 and it ended up being the chosen one. A viable back-up for this transfer would have happened in October 2012, since the basic features of "$2 + dV\,EGA$" repeat every 13 months. Regarding the interplanetary trajectory constraints, they could be divided into three categories:

- **Launch energy $C_3$ and timing constraints.** Fixing an initial value for the energy provided by the launcher, different possibilities of departure date could be analyzed. Every launch date defined a trajectory that was characterized by a required $C_3$ and deterministic $\Delta V$. The maximum $C_3 = 31.1$ km$^2$/s$^2$ was defined by the Atlas V551 launcher[2]. Analyzing Juno's ephemeris for the actual launch date, the calculated value is $C_3 = 31.08$ km$^2$/s$^2$. The trajectory reconstructed through the optimization problem and explained in subsection 2.1.2, revealed a value of $C_3 = 29.34$ km$^2$/s$^2$, with departure date on 18$^{\text{th}}$ August 2011. Restricting the launch window domain around 5$^{\text{th}}$ August 2011 (the actual one) the value is $C_3 = 30.40$ km$^2$/s$^2$. In the non-restricted window for departure, the trend of the $C_3$ over time can be evaluated in the work of Kowalkowski and Lam[1].

- **Interplanetary events.** The milestones of this phase were DSMs and EGA. The fly-by was constrained to happen at a fixed altitude of 800 km well above ISS, but it could be lowered up to 500 km. This last decrease of the altitude value could have improved the robustness of the trajectory in the case of eventual delays in DSMs, decreasing also the $\Delta V$ of the mission and the intensity of the radiation at Jupiter arrival[3]. However, the most challenging task was the selection of the DSM dates, in fact this choice would have affected the required launch $C_3$ and overall mission $\Delta V$[1]. Moreover, DSM had to be split into two equally lasting burns, separated by two days. This was dictated by engine capabilities, described in subsection 2.2.1. As precaution, due to anomalous pressure and temperature values of the oxidizer feeding line during DSM-1, the two manoeuvres ended up being performed two weeks apart. An additional problem arose from the $2 + dV\,EGA$ interplanetary structure and the needs to perform the DSM at aphelion while having real-time visibility. This constraint was set up by imposing a SEP angle greater than 10° for acquisition of data, and SEP angle greater than 3° for execution of the manoeuvre. This difference was due to the need of seven days to plan the manoeuvre on ground after the necessary two days of data collection. In the eventuality of a burn before solar conjunction, an adequate time to retry failed attempts was considered. Another constraint regarding telecommunications and navigation was due to the positioning of the toroidal antenna (TLGA) which is used for ground link in the early phases and is mounted on the aft deck and aligned with the -Z-axis, as shown in Figure 2.7. To ensure a good signal with this antenna, the ELA was constrained to be within ± 10° around 90°: since Doppler data is of very little value when ELA is too close to 90°, the combined range for the ELA resulted to be of 80° ÷ 87° and 93° ÷ 100°.

- **Jupiter arrival timing and geometry.** Jupiter arrival and insertion was constrained by multiple aspects. First of all, since a direct injection into the science orbit would have been too expensive, the burn was split into two manoeuvres (JOI and PRM), saving over 170 m/s[1] related to gravity losses. In order to avoid longitudes at which the magnetic field is stronger, JOI and PRM dates had to be accurately selected. In addition, due to the critical nature of JOI, the manoeuvre had to take place during the overlapping coverage of two DSN complexes. Since the longest one was provided by Goldstone-Canberra, the burn and pre-burn events had to happen during that time frame. As far as PRM was concerned, dual DSN coverage was not required. However, the optimal date for PRM could be selected in order to minimize the overall $\Delta V$ and to manoeuvre at lower magnetic field longitudes. Lastly, the perijove was bounded to be at distances higher than 4500 km over the 1 bar pressure level of the atmosphere, allowing to operate in the hole of the torus that describes the highest radiation levels.

### 2.1.2 Simulation of the interplanetary trajectory

To reconstruct the interplanetary phase, a simulation was set up in *Matlab*. The implemented model considered three heliocentric legs, linked with the patched-conics method:

- from Earth to DSM position;

- from DSM position to fly-by at Earth;
- from fly-by position to Jupiter.

In order to minimize the total $\Delta V$ of the mission, a cost function was defined. This is determined by the sum of four contributions:

- $\Delta V_{esc,E}$: escape from Earth heliocentric orbit into the first interplanetary leg;
- $\Delta V_{dsm}$: deep space manoeuvre;
- $\Delta V_{fb}$: burn manoeuvre at Earth's fly-by hyperbola pericentre;
- $\Delta V_{inj,J}$: injection into Jupiter's heliocentric orbit.

The calculations were based on analytical ephemeris for the planets and the Lambert method was used to design the paths. The implementation was constrained by various inputs, according to the development of the mission:

- Earth departure date, defined in the interval from 05/08/2011 to 26/08/2011
- DSMs condensed in one impulsive burn
- DSM date, from 20/08/2012 to 10/09/2012
- DSM position domain constrained by means of keplerian parameters from the real mission ephemeris
- Fly-by date, from 20/09/2013 to 20/10/2013
- Fly-by altitude, of at least 500 km
- Jupiter arrival date, from 20/06/2016 to 10/07/2016

Then a genetic algorithm was used to minimize the cost function and the match between the calculations and Juno ephemeris was verified as shown in Figure 2.6.
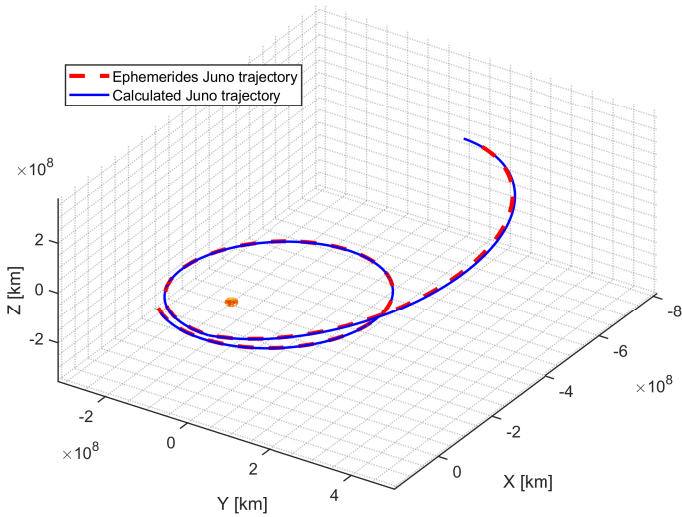


| | $\Delta V$ [km/s] | Date |
|---|---|---|
| **ESC$_E$** | 5.3920 | 14/08/2011 |
| **DSM** | 0.7225 | 29/08/2012 |
| **FB** | $1.9872 \cdot 10^{-7}$ | 08/10/2013 |
| **INJ$_J$** | 5.4552 | 09/07/2016 |

Table 2.3: Calculated solution

Figure 2.6: Comparison of trajectories

The obtained results are coherent with the actual mission data[4]. Regarding Table 2.3, some values might seem particularly high in relation to the main engine capabilities. Indeed, not all of the $\Delta V$s had to be performed by the main engine:

- $\Delta V_{esc,E}$ was executed by the upper stage of the Atlas V551, in the limits of the launcher performance $C_3$.
- $\Delta V_{inj,J}$ was due to the rendezvous at Jupiter. The only burn required to enter an elliptical orbit had to be given at the pericentre of the hyperbola. The impulsive $\Delta V$ can be calculated as follows, considering $e_{cap} = 0.9884$ and $r_p = 75237.6$ km in relation to the designed 107 days orbit:

$$\Delta V_{JOI} = v_\infty \left( \sqrt{1 + \frac{2\mu_J}{r_p v_\infty^2}} - \sqrt{\frac{\mu_J(1 + e_{cap})}{r_p v_\infty^2}} \right) = 424.07 \text{ m/s} \tag{2.1}$$

Moreover, the low $\Delta V_{fb}$ value in Table 2.3 indicates that gravity assist was not powered. Clean-up manoeuvre and TCMs were performed before and after the fly-by, hence this small burn.

### 2.1.3 $\Delta V$ budget

A summary of the planned, performed and simulated manoeuvres is exposed in Table 2.4. The design column is referred to the pre-launch schedule, while the performed column is relative to the actual mission. The designed mission never saw life since various problems occurred during the cruise phase: from a nominal capture orbit with a period of 107 days and a science orbit of 11 days, the new scheduled orbits were of 53.5 days and 14 days respectively.

For this precise reason the performed values differ from the design ones, especially the JOI, which was related to a different capture orbit, and the PC, which was not meant to be performed originally. The whole simulation has been performed on the designed 107 days orbit and the 11 days one. The final two columns show the required ME burn times for the designed and the performed mission respectively.

| Manoeuvres | Design [m/s] | Perf. [m/s] | Sim. [m/s] | $\tau_{ME}$ Design [min] | $\tau_{ME}$ Perf. [min] |
|---|---|---|---|---|---|
| TCM-1 ÷ 2 (RCS)[5] | 4.4 | 1.71 | - | - | - |
| DSM-1 (ME)[5] | 360.1 | 344.16 | 722.51 | 30.97 | 29.71 |
| DSM-2 (ME)[5] | 394.8 | 387.94 | | 30.07 | 29.77 |
| TCM-4 ÷ 15 (RCS)[5] | 32.5 | 7.89 | - | - | - |
| MEF (ME)[5] | 3.3 | 3.3 | - | - | - |
| JOI (ME)[6] | 424.07 $^I$ | 541.73 | 424.07 | 27.86 | 35.65 |
| JOI clean-up (RCS)[6] | 4.92 | 6.39 | - | - | - |
| PRM (ME)[6] | 636 | - | 602.45 | 35.19 | - |
| OTM pre-PC (RCS)[7] | 120 $^{II}$ | 94.88 | - | - | - |
| PC (RCS) | - | 56.39 | 69.97 $^{III}$ | - | - |
| OTM post-PC (RCS) | - | 108.08 | - | - | - |
| De-Orbit (RCS)[8] | 75 $^{IV}$ | 30.89 $^V$ | 87.93 | - | - |

Table 2.4: Overall mission budget and simulation

$^I$    This value has been assumed equal to the one calculated from the insertion on the 107 days orbit.
$^{II}$   This value assumes 30 nominal science orbits with a required $\Delta V$ of 4 m/s.
$^{III}$  This value is referred to the plane change of the 53 days orbit as no other trajectories required this manoeuvre.
$^{IV}$  This value is assumed equal between the 11 days orbit and the 14 days orbit.
$^V$    This value has been updated from the nominal 75 m/s since the de-orbit manoeuvre will be performed from a 53 days orbit and not from a 14 days orbit.

## 2.2 Propulsion system architecture

The spacecraft axes are defined as shown in Figure 2.7: the spacecraft is spinning along the +Z-axis, aligned with the HGA. The +X-axis is aligned with the MAG boom while the +Y-axis is in the direction of cross product between +Z-axis and +X-axis.
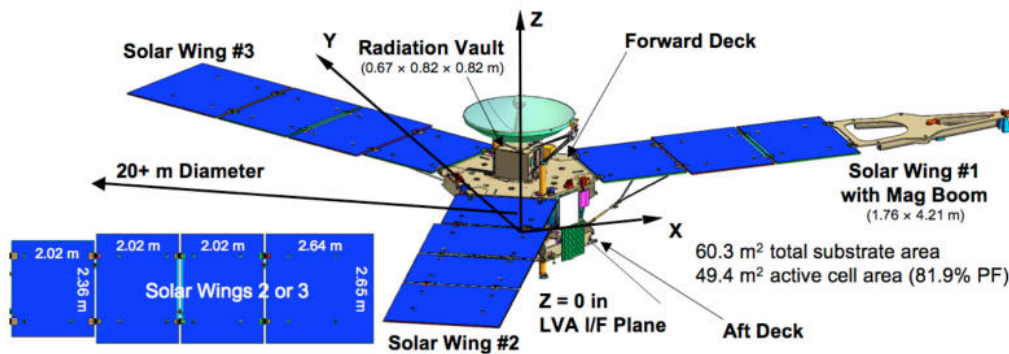


Figure 2.7: Axis description

### 2.2.1 Main Engine and RCS

Juno is equipped with a dual-mode propulsion system: the bi-propellant ME uses the hypergolic couple hydrazine and nitrogen tetroxide ($N_2H_4 - N_2O_4$) while RCS uses hydrazine as monopropellant. This choice was made to simplify the design: fewer tanks are needed as fuel ones are shared between the two systems. Moreover, the choice of this specific hypergolic couple is dictated by the storage requirements of the mission: in a five-year cruise, reliability and sturdiness of the propulsive system were among the main drivers of the mission. Electric thrusters were discarded as TRL-9 technologies were required: other limitations such as power budget, an highly radioactive environment, weight and space inside the spacecraft required a more simple and light solution.

The ME is a Leros 1b, built by Nammo[9], which produces about 662 N of thrust with $I_{s,me}$ = 318.6 s. This particular engine is certified for a 42 minutes continuous burn and has a cumulative lifetime of 342 minutes, so the manoeuvres shown in Table 2.4 are compliant with this constraint. This engine is utilized during the DSMs, JOI and PRM. It is mounted inside the body of the spacecraft along the -Z-axis, centred between the propellant tanks and under the electronic vault. This solution has probably been adopted due to space requirements inside the Atlas V fairing and safety precautions during the cruise phase. The ME is also shielded by a hatch that opens when a manoeuvre is needed. The RCS is used for TCMs, attitude control and general SK. The catalyst used to decompose the hydrazine is the S-405, based on iridium and aluminum[10]. The whole RCS is composed by four REMs, each of them mounted along the ±Y-axis on a pylon, as shown in Figure 2.8. Every pylon houses three thrusters, the MR-111C by Aerojet Rocketdyne[11], pointed in different directions, each providing a thrust of 4.5 N with $I_{s,rcs}$ = 220 s. Electrical power is required to operate the feeding valves, heating valves and the catalytic bed, amounting to a maximum of around 13 W[12].



Figure 2.8: Forward and Aft deck view

The pylons are raised respectively by 74 cm on the forward deck and about 26 cm on the aft deck as shown in Figure 2.9. With the need of limiting even more the interaction of the exhaust gasses with the on board instruments, the HGA and solar panels, axial thrusters are canted 10° away from the Z-axis while the lateral thrusters are canted 5° away from the X-axis and 12.5° toward the Z-axis[5]. This particular configuration of RCS is required since no RW nor any other type of active attitude control is present on the spacecraft: the ability of decoupling the forces and the momentum was thus needed. Lateral thrusters are denominated with letter "L" while axial thrusters are denominated with letter "A", as can be seen both from Figure 2.8 and Figure 2.9. This configuration increased the overall



Figure 2.9: RCS Forward mount

sturdiness of the propulsion system as "A" thrusters could be used as replacement of the ME for small manoeuvres. A simplified scheme of the propulsion system has been developed in Figure 2.10.

## 2.2.2 Manoeuvre Implementation Modes

Juno's manoeuvres can be performed in two different modes: *vector-mode* and *turn-burn-turn*.

The *vector-mode* consists of separated and coordinated axial and lateral burns from RCS thrusters. As seen in subsection 2.2.1, the thrusters are not exactly perpendicular one to the other, so during a *vector-mode* manoeuvre an induced axial $\Delta V$ is generated and must be compensated.

The *turn-burn-turn* mode consists in a sequence of RCS and ME burns: first the spacecraft slews to the design spinning rate of 5 RPM, then the ME is ignited and the manoeuvre is performed. At last, the spacecraft slews back to its nominal spinning rate. This mode is used during all the ME burns. In this kind of manoeuvre the RCS uses the "L" thrusters on the REMs.

### 2.2.3 Tanks

Juno's tanks are equally distributed throughout its hexagonal shaped body. Four tanks are needed to store hydrazine and two tanks are needed to store the oxidizer. As can be seen from Figure 2.9, the oxidizer ones (green tanks) are located along the X-axis, while fuel ones (blue ones) are placed in the remaining bays. All six tanks work at 2.15 MPa, estimated as the sum of the nominal operational pressure of the ME and a small amount, 50 kPa, induced by the pressure losses of the system[9]. On board tanks have a sphere-like shape: it allows to have the most internal volume with the lowest possible surface and so both weight and heat exchange are limited.

The two tanks[13] containing the supercritical helium needed to pressurize the propellant system are assumed to be initially pressurized at 21.5 MPa, a value ten times higher than the nominal working pressure, and are placed near solar wing one and solar wing two. Unlike fuel and oxidizer tanks,



Figure 2.10: Propulsion system architecture

helium ones do not have a sphere-like shape due to volume management inside the bays[14]: cylindrical tanks allow to fill better the gaps present under the main tanks. The positioning of the pressurizer tanks breaks even more the symmetry of the mass distribution: this feature, in concomitance with the distribution of the propellant tanks, will make the COM shift not only along the Z-axis unless other precautions were made in placing other internal components.

A system of valves regulates the pressure inside the tanks to allow nominal operations of the ME and RCS. All the tanks are insulated from their surroundings and heating elements are present on both tanks and feeding lines to ensure safe and nominal temperature inlet for the whole propulsion system. One of the main problem with managing liquid in space is the need of guiding the propellants to the feeding lines of the engines to avoid mixture of gas and liquids during the injection in the combustion chamber, compromising the correct functioning of the propulsion system. Moreover, liquid propellants produce sloshing movements that could apply forces and moments inside the tanks, causing an unsteady oscillatory spin. Juno is a spin-stabilized spacecraft so the induced forces would cause a movement of nutation. A Propellant Expulsion Device (PED) is thus needed: the spinning of the spacecraft helps guiding the propellant to the most exterior part of the tanks were feeding lines are located[15]. MEFs are tasks needed to flush the main propellant line in order to test the system after a long period of rest. In order to accomplish its mission, Juno holds about 2000 kg of propellant: about 1280 kg of fuel and 720 kg of oxidizer[5]. A more detailed analysis of tanks will be conducted in subsection 2.3.1.
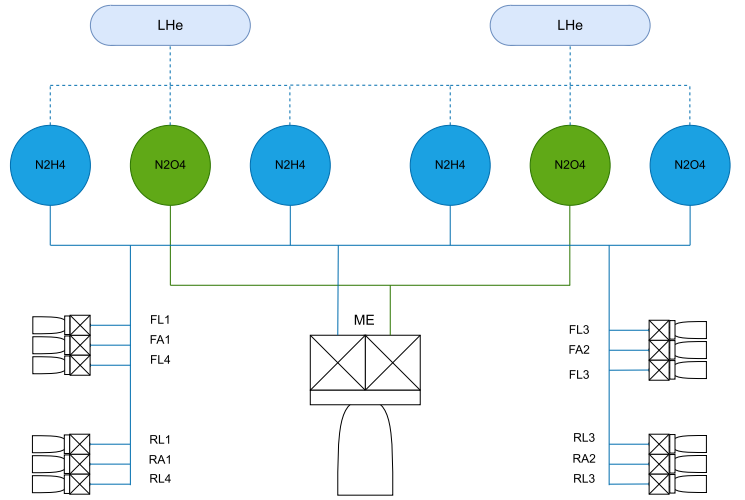
## 2.3 Reverse engineering of propulsion system

As described in subsection 2.2.3, the propulsion system counts four tanks for storing hydrazine, two tanks for storing NTO and two tanks for storing helium. To better understand the reasoning behind this choice, a reverse sizing for both the propellants and the pressurizer has been conducted given the data on the engines, the $\Delta V$ highlighted in Table 2.4 and the total dry mass $M_{dry}$[16] of the spacecraft. The whole process has taken into account the standardized margins from ESA.[17] Since the actual mission has greatly deviated from its initial design, a second propellant sizing was also performed on the real manoeuvres up to 7th June 2021[5][6][18] plus the required de-orbit to check the compliance with the design masses.

### 2.3.1 Fuel and oxidizer tanks sizing

1. To estimate the masses of the propellants, Tsiolkovsky rocket equation has been applied iteratively on the $\Delta V$ of the first column of Table 2.4. This process needs the dry mass $M_{dry} = M^{(0)}$ of the spacecraft as first input and starts from the last $\Delta V$ (the de-orbit burn) incrementing the computed total mass $M^{(i)}$ and the propellant mass $M_{p,me}^{(i)}$ or $M_{p,rcs}^{(i)}$ after each iteration.

$$M_{p,me}^{(i+1)} = M^{(i)} \cdot \left[ \exp\left( \frac{1.05 \cdot \Delta V^{(i)}}{I_{s,me} \cdot g_0} \right) - 1 \right] + M_{p,me}^{(i)} \tag{2.2}$$

$$M_{p,rcs}^{(i+1)} = M^{(i)} \cdot \left[ \exp\left( \frac{2 \cdot \Delta V^{(i)}}{I_{s,rcs} \cdot g_0} \right) - 1 \right] + M_{p,rcs}^{(i)} \tag{2.3}$$

$$M^{(i+1)} = M^{(i)} + M_{p,me}^{(i)} \qquad \text{or} \qquad M^{(i+1)} = M^{(i)} + M_{p,rcs}^{(i)} \tag{2.4}$$

where the respective formula is applied based on which engine type performs the i-th manoeuvre.

2. From the final $M_{p,me}$ and $M_{p,rcs}$, the masses of fuel and oxidizer are then computed. This is done by knowing the nominal $O/F$ ratio (0.85) of the ME[9] and that the RCS only uses hydrazine as propellant. Exploiting the density of the propellants, the total volumes for fuel and oxidizer are retrieved.

$$M_f = \frac{1}{O/F + 1} \cdot M_{p,me} + M_{p,rcs} \tag{2.5}$$

$$M_{ox} = \frac{O/F}{O/F + 1} \cdot M_{p,me} \tag{2.6}$$

The estimated masses are rather similar to the real ones, as it can be seen in Table 2.5.

|  | Estimated masses [kg] | Real masses [kg][16] | Relative error [%] |
|---|---|---|---|
| $M_f$ | 1309.5 | 1280 | 2.304 |
| $M_{ox}$ | 751.9 | 752 | 0.013 |

Table 2.5: Comparison between estimated and real masses

3. Having the total volumes of propellants, they have been split among the number of spherical tanks. Since the radius $r_{tank}$ obtained for the two types of tanks are very similar and having two different tanks is inconvenient, the larger one was selected.

| Fuel tank radius [cm] | Oxidizer tank radius [cm] |
|---|---|
| 43.99 | 40.91 |

Table 2.6: Comparison between obtained radii

4. The pressure of the tanks $p_{tank}$ is kept constant (as described in subsection 2.2.3). From the pressure and the volume of one tank, the required thickness $t_{tank}$ can be computed by choosing the material, characterized by its density $\rho$ and its tensile yield strength $\sigma$.

$$t_{tank} = \frac{r_{tank} p_{tank}}{2\sigma} \tag{2.7}$$

5. The dry mass of one tank is then computed to select the material:

$$M_{tank} = \frac{4}{3}\pi\rho \left[ (r_{tank} + t_{tank})^3 - r_{tank}^3 \right] \tag{2.8}$$

Three different materials have been taken into consideration, and the lighter configuration has been selected.

|  | Ti6Al4V | Al7075 | Stainless steel |
|---|---|---|---|
| $\sigma$ [MPa] | 950 | 510 | 1400 |
| $\rho$ [kg/m³] | 4500 | 2810 | 8100 |
| $t_{tank}$ [mm] | 0.50 | 0.93 | 0.34 |
| $M_{tank}$ [kg] | 5.45 | 6.35 | 6.66 |

Table 2.7: Properties of the materials tested for the sizing of the tanks

### 2.3.2 Pressurizer tanks sizing

1. As a first approximation, the pressure for the helium tanks is supposed to be ten times the pressure for the propellant tanks $p_{tank}$, and helium is considered to be a perfect gas (actually it is in a supercritical state). The temperature $T_{tank}$ for the tanks is assumed to be 20 °C. Starting from these assumptions, the mass and the volume

of the total required helium are computed as follows:

$$M_{He} = 1.2 \cdot \frac{p_{tank} \cdot 6V_{tank} \cdot \gamma_{He}}{(1 - 1/10) R_{He} T_{tank}} \tag{2.9}$$

$$V_{He} = \frac{M_{He} R_{He} T_{tank}}{10 p_{tank}} \tag{2.10}$$

2. Since the two tanks are cylindrical, the geometry is undefined given only the volume of one tank. To add the missing constraint, a minimization of the total surface is assumed, which can minimize the internal stress due to pressure and the heat transfer through the walls (subsection 2.2.3).

$$r_{tank,He} = \left( \frac{1/2 V_{He}}{2\pi} \right)^{1/3} \tag{2.11}$$

$$h_{tank,He} = \frac{1/2 V_{He}}{r_{tank,He}^2 \pi} \tag{2.12}$$

3. As already done in subsection 2.3.1, the thickness $t_{tank,He}$ is computed for the materials in Table 2.7 as:

$$t_{tank,He} = \frac{r_{tank,He} \cdot 10 p_{tank}}{2\sigma} \tag{2.13}$$

4. The dry mass of one tank is then computed to select the material:

$$M_{tank,He} = \rho \, h_{tank,He} \, \pi \left[ (r_{tank,He} + t_{tank,He})^2 - r_{tank,He}^2 \right] + 2 \rho \, t_{tank,He} \, r_{tank,He}^2 \, \pi \tag{2.14}$$

As for the propellants tanks, titanium alloy appears to be the lightest solution (Table 2.8). This is the material most likely used for the tanks on the real satellite, and it is the most widely used in space due to its high strength to mass ratio and corrosion resistance.

|  | **Ti6Al4V** | **Al7075** | **Stainless steel** |
|---|---|---|---|
| $t_{tank,He}$ [mm] | 3.58 | 6.68 | 2.43 |
| $M_{tank,He}$ [kg] | 30.62 | 35.73 | 37.51 |

Table 2.8: Thickness and mass of helium tanks for different materials

### 2.3.3 Computation of actual propellants usage

The second sizing relies on the same procedure highlighted in subsection 2.3.1 with the difference that it starts from the launch mass $M_{launch} = M^{(0)[16]}$ and considers the $\Delta V$ from the second column of Table 2.4 in chronological order. Equation 2.2 and Equation 2.3 are thus modified as follows:

$$M_{p,me}^{(i+1)} = M^{(i)} \cdot \left[ 1 - \exp\left( \frac{-\Delta V^{(i)}}{I_{s,me} \cdot g_0} \right) \right] + M_{p,me}^{(i)} \tag{2.15}$$

$$M_{p,rcs}^{(i+1)} = M^{(i)} \cdot \left[ 1 - \exp\left( \frac{-\Delta V^{(i)}}{I_{s,rcs} \cdot g_0} \right) \right] + M_{p,rcs}^{(i)} \tag{2.16}$$

where the ESA margins[17] were not applied since the actually performed manoeuvre values were utilized. The real and consumed masses are reported in Table 2.9.

|  | **Real masses [kg]** | **Consumed masses [kg]** | **Remaining masses [kg]** |
|---|---|---|---|
| $M_f$ | 1280 | 986 | 294 |
| $M_{ox}$ | 752 | 560 | 192 |

Table 2.9: Real and consumed propellants masses

The *remaining masses* column denotes the propellants masses still present in the spacecraft as of 7th June 2021, which are obtained by subtracting the calculated masses from the real ones. Since the de-orbit is mandatory its $\Delta V$ has been considered as a final real manoeuvre even though it hasn't happened yet.

# Bibliography

[1] Try Lam Theres D. Kowalkowski. "Launch Period Development for the Juno Mission to Jupiter". In: (2008).

[2] United Launch Alliance. *Atlas V Juno*. Site: `https://www.ulalaunch.com/docs/default-source/rockets/atlasvusersguide2010a.pdf?sfvrsn=f84bb59e_2`. 2011.

[3] Rick Nybakken. "The Juno Mission to Jupiter: A pre-launch update". In: (2011).

[4] Paul F. Thompson et al. "Juno navigation for Jupiter orbit insertion". In: (2017).

[5] Thomas A. Pavlak et al. *Maneuver Design for the Juno Mission: Inner Cruise*. AIAA space forum. Site: `https://arc.aiaa.org/`. 2018.

[6] Paul W. Stumpf et al. *Maneuver Operations During Juno's Approach, ORBIT INSERTION, AND EARLY ORBIT PHASE*. JPL open repository. Site: `https://dataverse.jpl.nasa.gov/file.xhtml?fileId=58768&version=1.1&toolType=PREVIEW`. 2017.

[7] S. Stephens. *Juno Mission Plan Document*. Planetary Data System. Site: `https://pds.nasa.gov/ds-view/pds/viewMissionProfile.jsp?MISSION_NAME=JUNO`. 2011.

[8] Various. *Juno Mission and Trajectory Design*. Website. Site: `https://spaceflight101.com/juno/juno-mission-trajectory-design/`. 2024.

[9] Nammo. *Leros 1b engine*. Journal of Geophysical Research: Planet. Site: `https://www.nammo.com/wp-content/uploads/2021/03/2021-Nammo-Westcott-Liquid-Engine-LEROS1B.pdf`.

[10] Dr. Edward. J. Wucherer al. *Improving and Testing S-405 Catalyst*. AIAA space forum. Site: `https://arc.aiaa.org/doi/epdf/10.2514/6.2013-4053`. 2013.

[11] *Aerojet Rocketdyne Propulsion plays role in Juno mission*. Online Communication. Site: `https://www.proquest.com`. 2016.

[12] *MR-111C datasheet*. Site: `http://www.astronautix.com/m/mr-111.html`.

[13] *Launch*. Site: `https://www.missionjuno.swri.edu/launch`.

[14] Dr. Mary M. Mellott et al. *NSSDCA/COSPAR ID: 2011-040A*. Nasa SSDCA. Site: `https://nssdc.gsfc.nasa.gov/nmc/spacecraft/display.action?id=2011-040A`. 2022.

[15] Sathya Gangadharan et al. *Modeling of Fuel Slosh in a Spin Stabilized Spacecraft with On-Axis Propellant Tanks Implemented with Diaphragms*. AIAA Modeling and Simulation Technologies Conference 10 - 13 August 2009, Chicago, Illinois. Site: `https://arc.aiaa.org/`. 2009.

[16] NASA JPL. *Juno Quick Facts*. Site: `https://www.jpl.nasa.gov/news/press_kits/juno/facts/`. 2011.

[17] European Space Agency. "Margin philosophy for science assessment studies". In: (2012).

[18] Thomas A. Pavlak et al. "Juno trajectory redesign following PRM cancellation". In: (2017).

# Homework 3

## Notation

| | | | | |
|---|---|---|---|---|
| **TMTC** | Telemetry and Telecommand | | **BVR** | Block-V Receivers |
| **HGA** | High Gain Antenna | | **FTS** | Frequency and Timing Subsystem |
| **MGA** | Medium Gain Antenna | | **BER** | Bit Error Rate |
| **LGA** | Low Gain Antenna | | **MWR** | Micro Wave Radiometer |
| **TLGA** | Toroidal Low Gain Antenna | | **DSS** | Deep Space Station |
| **TWTA** | Traveling Wave Tube Amplifier | | **RSR** | Radio Science Receiver |
| **ALGA** | Aft Low Gain Antenna | | **D/L** | Downlink |
| **FLGA** | Forward Low Gain Antenna | | **U/L** | Uplink |
| **DSN** | Deep Space Network | | $P_{rx}$ | Power received [W] |
| **DSM** | Deep Space Manuevers | | $P_{tx}$ | Power transmitter [W] |
| **JOI** | Jupiter Orbit Insertion | | $G_{rx}$ | Gain receiver [-] |
| **PRM** | Period Reduction Manuever | | $G_{tx}$ | Gain transmitter [-] |
| **SDST** | Small Deep Space Transponder | | $L_c$ | Cable losses [-] |
| **SSPA** | Solid State Power Amplifier | | $L_s$ | Space losses [-] |
| **DPM** | Digital Processing Module | | $L_{p,tx}$ | Receiver pointing losses [-] |
| **F1** | Fundamental frequency | | $L_{p,rx}$ | Transmitter pointing losses [-] |
| **DOR** | Differential One-way Ranging | | $L_a$ | Atmospheric losses [-] |
| **RHCP** | Right-Hand Circular Polarization | | $L_{cv}$ | Antenna cover losses [-] |
| **LHCP** | Left-Hand Circular Polarization | | $k$ | Boltzmann constant [J/K] |
| **RF** | Radio Frequency | | $T_{eq}$ | Equivalent temperature [K] |
| **OTM** | Orbit Trim Manuever | | $R$ | Datarate [bps] |
| **BPSK** | Binary Phase Shifting Keying | | $N_0$ | Noise spectral density [W/Hz] |
| **MFSK** | Multiple Frequency Shift Keying | | $E_b$ | Energy per bit [J/bit] |
| **AWVR** | Advanced Water Vapor Radiometer | | $r_{JE}$ | Juno-Earth distance [AU] |
| **LNA** | Low Noise Amplifier | | $f$ | Frequency [Hz] |
| **KaTS** | Ka-band Translator | | $d_g$ | Ground antenna diameter [m] |
| **IF** | Intermediate Frequency | | $\eta$ | Pointing error [-] |
| **RF** | Radio Frequency | | $G$ | Antenna gain [dB] |
| **RS** | Radio Science | | $\theta_{bw}$ | Antenna beamwidth [deg] |
| **SR** | Science Receiver | | $EIRP$ | Equivalent isotropic radiated power [dBm] |
| **OLR** | Open Loop Receivers | | $(.)_{mar}$ | Margin value |
| **VLBI** | Very Long Baseline Interferometry | | | |

## 3.1 TMTC system architecture

The Juno TMTC subsystem purpose is to communicate data about the status of the spacecraft, to send scientific data and to receive commands, from and to the DSN antennas. Both the uplink and downlink are performed in X-band frequency: 8.4 GHz for downlink and 7.1 GHz for uplink. The selection of this band was imposed by pre-existing DSN facilities. It allows to transmit relatively large datarates over wide distances with low atmospheric attenuation. One of the main goals of the mission is to study Jupiter's gravity field: this is accomplished by exploiting the difference in Doppler effect of the telecommunication from the model and the real jovian gravity field. Due to the harsh environment that Juno faces and the need to measure precisely the residual frequency, transmission on both X-band and Ka-band during gravity science is needed. The Ka-band has an advantage on the X-band since the noise due to



Figure 3.11: Location of telecommunication antennas

interplanetary plasma is inversely proportional to the wavelength, higher on the Ka-band, making the measurements more accurate[1]. For this reason, the HGA can operate in 3 different modes:

- **X/X**: uplink and downlink are coherent and performed in X-band;

- **X/X & X/Ka**: simultaneous transmission on X-band (uplink and downlink), together with a coherent Ka-band downlink at 32 GHz and X-band uplink;

- **X/X & Ka/Ka**: phase coherent X-band uplink and downlink together with a phase coherent Ka-band uplink at 34 GHz and downlink.

In order to calibrate the dispersive noise contribution when receiving X-band and Ka-band signals simultaneously, Juno is equipped with a KaTS. This instrument is capable of receiving a Ka-band uplink unmodulated carrier from DSN and to generate a Ka-band downlink unmodulated carrier coherent with the uplink to maintain the phase stability from ground communication, on which the quality of the experiments depends[2].

Five antennas are mounted on-board Juno with different orientations, positions and capabilities: one HGA, one MGA, two LGAs and one TLGA.

In order to process different signals at different frequencies, Juno has two SDSTs, capable of performing different tasks. The prime unit provides X/X and X/Ka link, whereas the secondary unit only operates on the single X-band. Each SDST is composed of four different units: the DPM, the down converter, the power converter and the exciter unit. The DPM is responsible for managing the data incoming from the down-converter, encoding them and providing X-band baseband telemetry. The down-converter module converts the incoming 7.1 GHz signal into an intermediate frequency at 4/3 F1, where F1, approximately 9.55 MHz, is the fundamental frequency from which up and downlink frequencies are derived. The power converter is responsible for supplying a steady voltage to all SDST modules and the exciter is responsible for taking as an input telemetry, DOR, ranging and for phase-modulating the downlink carrier[1][2].

The SDST is responsible for generating the X-band downlink carrier by coherently multiplying the frequency of the uplink carrier by a turn-around ratio of 880/749. All X-band signals are amplified by one of two-redundant 25 W TWTAs[2]. This kind of technology was imposed by the high power demand for the link on this frequency. For the Ka-band transmission, SSPA was preferred due to less required power for transmission and weight saving.

Before the transmission of the signal actuated by the antennas, the data is manipulated with modulation and encoding techniques. The chosen modulation is BPSK which ensures a good use of spectrum and relatively low BER. Moreover, it was flight-proven and requires less complex on-board architecture. Encoding is performed in two ways depending on the type of the transmission: the Reed-Solomon algorithm allowed lower BER to be reached, while Turbo code 1/6 was used for larger datarates of transmission.

### 3.1.1 HGA

The HGA[2][3] is the principal means of communication with Earth throughout most of the cruise and science mission. It is mounted on the forward deck, aligned with the spin axis of the spacecraft, as shown in Figure 3.11. Due to the significant distance between Juno and DSN antennas and the limited transmitter power, HGA gain maximization was a priority. Constraints on dish dimension and in the attitude control of the spin-stabilized spacecraft were present: the Atlas V fairing limited the HGA dish diameter to 2.5 meters, then the presence of massive solar arrays prevented pointing the main beam to anything tighter than about ± 0.25°. The latter limitation would have led to an insufficient gain in the HGA, preventing closing the link with Earth. The most limiting factor in designing
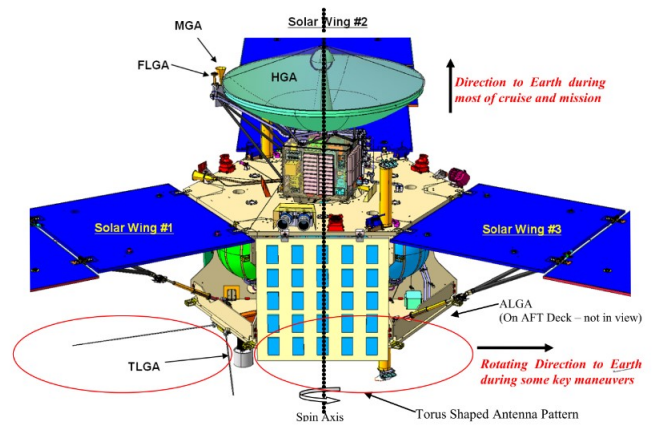
the HGA was the need of both transmitting and receiving on X-band and Ka-band without affecting excessively the performance of any signal. Because of these requirements, a dual-reflector Gregorian-style optics was installed. The latter consists in a parabolic main reflector and an elliptical sub-reflector, making the whole system low in mass and compact[3]. The outer annular region is made so that the radiated field of the X-band is 180° out of phase with the inner region aperture field: the resulted beamwidth of the Ka-band is approximately the same as the X-band one. This modification created almost no performance degradation on X-band link. Based on frequency and operational mode, different polarizations are utilized: X-band uses RHCP for both uplink and downlink, while Ka-band uses RHCP for downlink and LHCP for uplink[2]. Required gain is about 44 dB for the X-band in both uplink and downlink and around 47 dB for the Ka-band.

Other limiting factors were present in designing the HGA in terms of thermal and structural constraints: the stability in pointing at low temperatures is granted by a very stiff graphite composite. Moreover, the HGA's shielding from the high temperature oscillation (from -175°C to 135°C) and radiation dose experienced during both cruise and jovian phase is accomplished using a thermal blanket made of a carbon-loaded Germanium-Kapton material[3][4]. As a result, the performances were only affected by a loss of 0.25 dB at X-band and a 0.5 dB loss on the Ka-band.

### 3.1.2 MGA & LGAs

One MGA and two LGAs are mounted on-board Juno. Their position can be seen in Figure 3.11. Both types of antennas come as legacy from previous missions. LGAs were previously used on the Mars Reconnaissance Orbiter and as part of a family of antennas used for deep space missions. Instead, MGA was used in Mars Exploration Rover cruise stage[3].

The MGA is a conical horn-style antenna and it is aligned with the +Z-axis as the HGA and it is used during cruise, safe mode and manoeuvres. It is capable of both LHCP and RHCP for redundancy and communicates with the DSN only in X-band, using the same frequencies of the HGA. This antenna provides at least 18.1 dBic while receiving and 18.8 dBic while transmitting, with a 3 dB beamwidth of ± 10.3° and ± 9.3° respectively.

The two identical and coupled LGAs are pointing in opposite directions, one mounted on the forward deck (FLGA) and the other on the aft deck (ALGA). LGAs have a choked horn design and transmit on the same X-band frequencies as the MGA and HGA. While delivering inferior performances regarding the minimum required boresight (8.7 dB in receiving and 7.7 dB in transmitting), they operate with a higher 3 dB beamwidth at around ± 40°[2].

The LGAs are used mainly at a distance inferior to 0.5 AU from Earth and during manoeuvres, when orientation of the spacecraft does not allow HGA communications due to sun-pointing requirement. Throughout main engine burns, the MGA is used in sequence with HGA and TLGA. This suit of antennas is also used during MWR science configuration.

### 3.1.3 TLGA

The TLGA is placed on the aft deck of Juno, aligned with solar wing #1. This antenna works at the same X-band frequency of the other antennas but differs from them since it has a bi-conical horn design and it is able to produce a RHCP radial pattern around Juno's spin axis: this characteristic is needed to ensure continuous coverage during all critical events, such as the DSMs, JOI, PRM and OTMs, when the attitude does not allow for direct Earth pointing. This antenna transmits only in a carrier or subcarrier configuration, where no ranging nor telemetry signals are modulated onto the carrier. During ME manoeuvres Juno encodes MFSK tones by modulating a varying frequency subcarrier onto the carrier. Every subcarrier frequency is associated to a particular event or state of the spacecraft and allows a complete knowledge of Juno's health. The particular advantage of using a subcarrier is the capability of providing an additional channel of transmission: it allows different signals to be received together as one and then to be separated out by the receiver.

A toroidal antenna pattern can be produced by a dipole, but this design limits heavily the maximum gain reachable to around 2.2 dB, which is insufficient to provide communications between Juno and Earth. Thus, a bi-conical parabolic-shaped antenna with corrugated horn has been developed, allowing for a compact and efficient design: this configuration achieves values lower than 20 dB in return losses over the entire used X-band[3]. The RHCP pattern is achieved through a four-layer meander-line polarizer, built to minimize RF losses. As the HGA described in subsection 3.1.1, the TLGA is also covered in a Germanium-Kapton blanket to minimize high energy electrons' flux. Gains required for the TLGA are of 5.5 dBic while receiving and 6.5 dBic while transmitting, with a beamwidth of ± 10° in both reception and transmission at ± 90° with respect to the boresight angle[2].

### 3.1.4 Ground stations

In order to retrieve data, Juno relies on the antennas of NASA's DSN, a system of three complexes spread around the globe, separated by approximately 120° in longitude: one is located in Goldstone, California; one in Madrid, Spain; the last one in Canberra, Australia. This configuration allows for constant observation of spacecraft while Earth rotates, as can be visualized in Figure 3.12. Each site is fitted with one 70-meter diameter antenna and a set of 34-meter diameter antennas. At Ka-band, the beamwidth of the latter antennas is 4 times narrower than the X-band beamwidth (0.016° vs. 0.077° respectively), making the pointing critical to establish a stable link with the spacecraft.

All antennas are capable of receiving and transmitting in X-band, however only the smaller ones are also capable of receiving in Ka-band. DSS-25 antenna in Goldstone is the sole capable of Ka-band uplink: all Juno's closest approach periods to Jupiter are planned such that this particular antenna is in sight.

Since the troposphere introduces delays in the Doppler signal path, in order to retrieve a more accurate reading during gravity science, DSS-25 is equipped with a AWVR that measures the wet component of the troposphere and various frequencies, including 31.4 GHz, where Ka-band signal are performed. The wet component delays are statistically combined with data considering effects from surface meteorology to have a full evaluation of the delays in the Doppler signals[5].

During communications, the signal is received by the antennas and then amplified by the LNA into an IF (at 300 MHz) easier to be carried by cables rather than a RF, that needs waveguides. Depending on the flexibility needed, an open-loop or closed-loop or monopulse closed-loop can be used for signal processing. There have been three types of open-loop receivers during Juno era, all functioning in similar capacities: RSR, VLBI, WVSR. The last two have been recently replaced by a more recent OLR due to obsolescence issues in maintenance[6]. Open-loop receivers opt for a specific band of frequencies to amplify and then transmit the data to RS or VLBI equipment for processing and storage. They are used during high-dynamic or low-signal level events because of their ability to best guess the frequency of the received signal in order to sample the entire spectrum around the spacecraft's center frequency. Regarding closed-loop receivers, they are based on the advanced technology of BVRs, in which the spacecraft's downlink is selected and received. BVRs



Figure 3.12: DSN coverage

are able to detect subcarriers carrying telemetry or ranging data and to decode and process them. A program known as *conscan*[7] is in charge of observing the strength of the receiver's signal to optimize the antenna's pointing via small circular movements. The usage of *conscan* during VLBI or RS operations is discouraged due to variations in signal levels, in its place a monopulse closed-loop receiver is used to optimize Ka-band reception. The monopulse system compares the gain and the phase of the received Ka-band signal to estimate needed corrections in the antenna's pointing to improve signal-to-noise ratio by 1÷3 dB-Hz[1].

X-band and Ka-band signals are generated by the FTS, which relies on a hydrogen maser clock to maintain a stable reference frequency. The X-band exciter and Ka-band exciter generate an uplink carrier signal which is amplified by the transmitters. The Juno spacecraft then receives these signals and phase-coherently retransmits them to the DSN antenna. In Figure 3.13 it is possible to observe a simplified scheme of Juno's communication architecture.
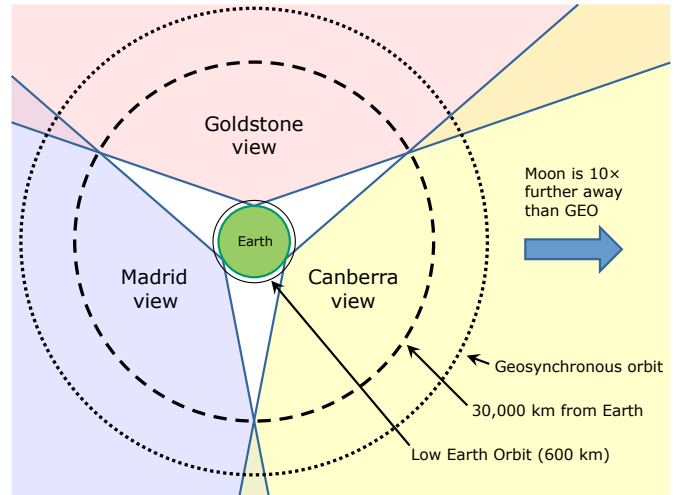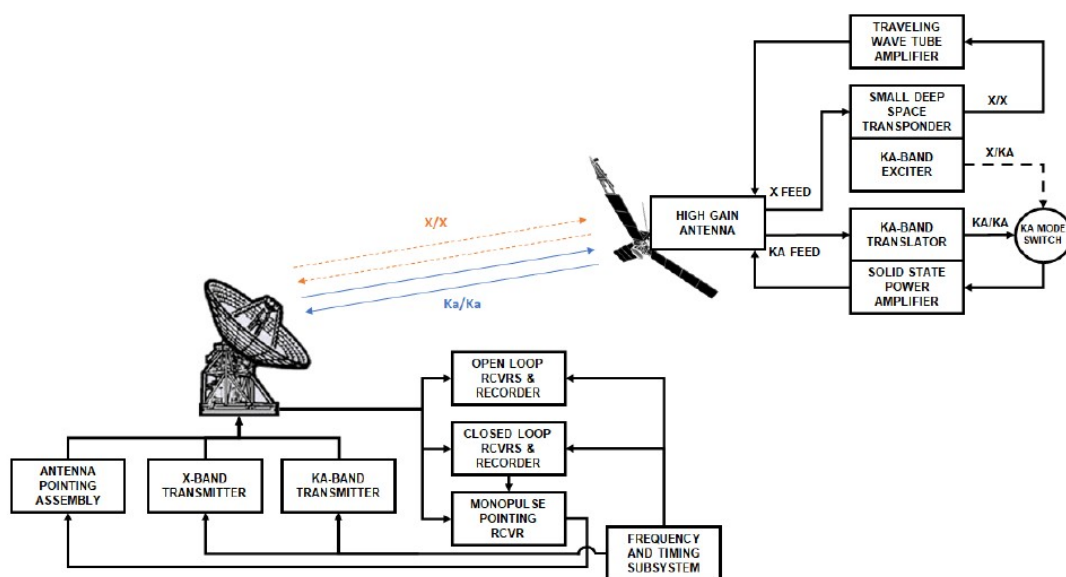


Figure 3.13: Ground Station and Juno communication scheme

22

## 3.2 Phases breakdown

The satellite utilizes all the antennas throughout the different phases of the mission. During each one, the TMTC system must satisfy different linking requirements. The main phases are depicted in time in Figure 3.14 and then briefly discussed in Table 3.10.
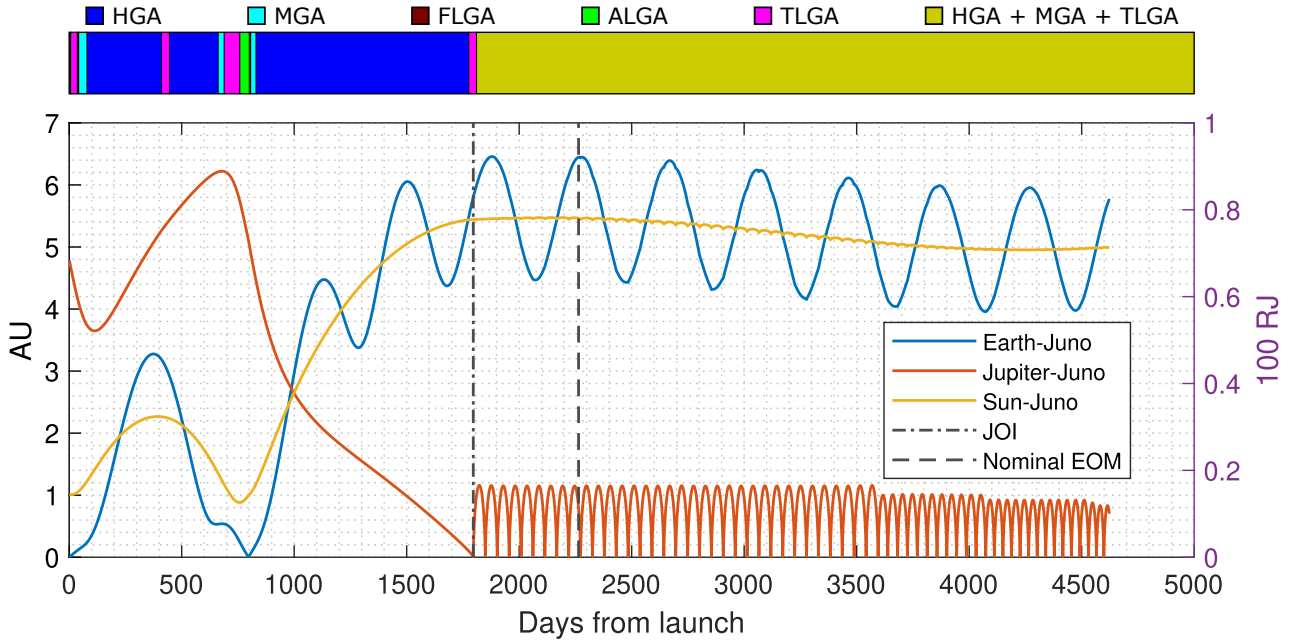


Figure 3.14: Antennas operability during mission

| Phase | Downlink/Uplink [bps] | Phase summary |
|---|---|---|
| Initial Acquisition | 1745 / - | Initial acquisition performed through LGAs (zoom on Figure 3.14). Reed-Solomon coding was used. |
| Cruise | 100 / 7.8125 | Ranging is on during the whole cruise. Since Juno has to point the Sun, HGA is not usable during fly-by so all the other antennas are sequentially employed (Figure 3.14). |
| Orbital Operations | $1.8 \cdot 10^4$ / 2000 | This is the most demanding phase, it requires at least 18 kbps in downlink through HGA. Also MGA and TLGA are used during OTMs, the latter only for tones (Figure 3.14). |
| Critical Event Coverage | - / - | No data during these phases, just tones through TLGA. |
| Safe Mode | 10÷40 / 7.8125 | Downlink datarate may be changed by flight software. Ranging is switched off during this mode. |

Table 3.10: Summary of data links during mission phases[2]

## 3.3 Reverse sizing of the HGA

The reverse sizing of the HGA is based on the link budget equation that represents a power balance between the transmitted signal and the receiver noise. The same equation can be applied on both uplink and downlink. It is valid for all the architectures, both that transmit data or tones.

$$\frac{P_{rx}}{N_0} = \frac{P_{tx}G_{tx}G_{rx}L_{tot}}{kT_{eq}} > \left(\frac{P_{rx}}{N_0}\right)_{min}$$

(3.17)

For antennas that broadcast data, an additional equation is used to constrain the sizing.

$$\frac{E_b}{N_0} = \frac{P_{tx}G_{tx}G_{rx}L_{tot}}{kT_{eq}R} > \left(\frac{E_b}{N_0}\right)_{min} \tag{3.18}$$

$L_{tot}$ considers the following losses:

$$L_{tot} = L_c \cdot L_s \cdot L_{p,tx} \cdot L_{p,rx} \cdot L_a \cdot L_{cv} \tag{3.19}$$

For each communication link, different minimum required ratios are defined. In particular, $\frac{E_b}{N_0}$ must also satisfy the Shannon theorem by ensuring a value higher than −1.59 dB. The HGA, as described in subsection 3.1.1, is used for the downlink of telemetry and scientific data during the science orbits around Jupiter. It has been sized in the following scenario:

- the maximum distance from Earth $r_{JE}$ = 6.5 AU;
- the minimum datarate $R$ = 18 kbps has to be ensured regarding the distance.

From the literature, some other parameters were recovered and reported in Table 3.11. The results of the sizing are shown in Table 3.12. In particular, some margin is present on both X-band and Ka-band. Since the X-band is the only one transmitting data, Figure 3.15 and Figure 3.16 focus on the margin of the downlink. The principal loss of the link is given by the distance, so the two design parameters have been described as a function of it.

|  | X-D/L | X-U/L | Ka-D/L | Ka-U/L |
|---|---|---|---|---|
| $f$ [GHz] | 8.4 | 7.1 | 34.4 | 32.1 |
| $R$ [kbps] | 18 | 2 | – | – |
| $d_{HGA}$ [m] | 2.5 | | | |
| $d_g$ [m] | 34 | | | |
| $P_{tx}$ [W] | 25 | $1.8 \cdot 10^4$ | 2.5 | $1.8 \cdot 10^4$ |
| $\eta_{HGA}$ [deg] | 0.25 | | | |
| $\eta_g$ [deg] | $4 \cdot 10^{-3}$ | | $2 \cdot 10^{-3}$ | |
| $L_c$ [dB] | −2 | – | −2 | – |
| $L_a$ [dB] | −0.2 | | −1.09 | |
| $L_{cv}$ [dB] | −0.25 | | −0.5 | |
| $T_{eq}$ [K] | 21 | 401.25 | 21 | 770.63 |
| $\left(\frac{P}{N_0}\right)_{min}$ [dB-Hz] | 43.64 | 49.13 | 26.50 | 42.57 |
| $\left(\frac{E_b}{N_0}\right)_{min}$ [dB] | −0.1 | 9.6 | – | – |

Table 3.11: HGA data for sizing[2]

|  | X-D/L | X-U/L | Ka-D/L | Ka-U/L |
|---|---|---|---|---|
| $G_{HGA}$ [dBi] | 44.25 | 42.79 | 56.50 | 55.90 |
| $G_g$ [dBi] | 66.93 | 65.47 | 79.17 | 78.57 |
| $\theta_{bw,HGA}$ [deg] | 0.932 | 1.10 | 0.438[I] | |
| $\theta_{bw,g}$ [deg] | 0.069 | 0.081 | 0.017 | 0.018 |
| $L_s$ [dB] | −290.63 | −289.17 | −302.88 | −302.28 |
| $L_p$ [dB] | −0.904 | −0.646 | −4.09 | −4.51 |
| $EIRP$ [dBm] | 85.98 | 138.02 | 87.98 | 151.12 |
| $N_0$ [dBm/Hz] | −185.38 | −172.57 | −185.38 | −169.73 |
| $P_{rx}$ [dBm] | −138.83 | −109.46 | −140.90 | −101.36 |
| $\frac{P}{N_0}$ [dB-Hz] | 46.55 | 63.11 | 44.47 | 68.38 |
| $\left(\frac{P}{N_0}\right)_{mar}$ [dB-Hz] | 2.91 | 13.98 | 17.97 | 25.81 |
| $\frac{E_b}{N_0}$ [dB] | 4.00 | 30.10 | – | – |
| $\left(\frac{E_b}{N_0}\right)_{mar}$ [dB] | 4.10 | 20.50 | – | – |

Table 3.12: Results for HGA

[I] This value was recovered from a graphical analysis of the HGA Ka-band gain pattern.[2]
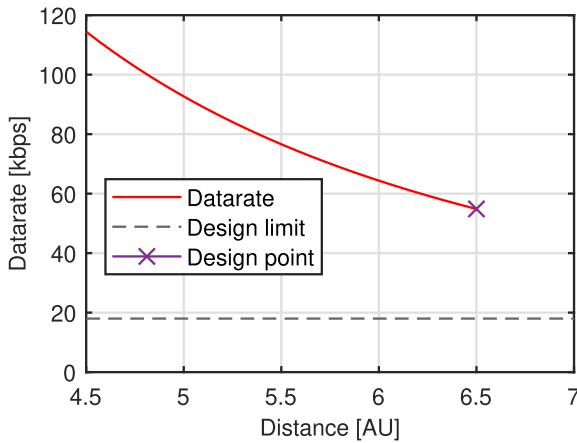


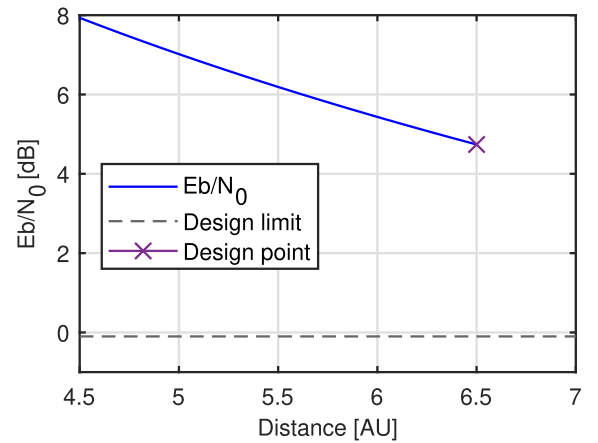Figure 3.15: Datarate as function of distance by fixing $E_b/N_0$ = -0.1 dB



Figure 3.16: Energy per bit to noise ratio as function of distance by fixing $R$ = 18 kbps

# Bibliography

[1] Dustin Buccino et al. "Juno Gravity Science: Five Years of Radio Science Operations with Ka-band Uplink". In: (2022).

[2] Anthony P. Mittskus et al. "Juno Telecommunications". In: (2012).

[3] Anthony P. Mittskus et al. "Telecommunications Antennas for the Juno Mission to Jupiter". In: (2012).

[4] *DuPont™ Kapton*. Site: kapton.com.

[5] Dustin Buccino et al. "Calibration and Performance of Juno Radio Science Data". In: (2020).

[6] Dustin Buccino et al. "Detecting Juno's "Heartbeat": Communications Support during Critical Events of the Juno Mission". In: (2020).

[7] *Deep Space Network*. Site: https://science.nasa.gov/learn/basics-of-space-flight/chapter18-3/.

# Homework 4

## Notation

| | | | |
|---|---|---|---|
| **SYM** | Explanation | **SYM** | Explanation |
| **SYM** | Explanation | **SYM** | **REFERENCE**[1] |

## 4.1 Introduction of AOCS

The Attitude and Orbital Control System of Juno comprehends various sensors and actuators that are vital to maintain the satellite in operability conditions and to execute all the basic tasks. In this chapter, the main modes of the satellite are deduced through the analysis of the mission already done in previous chapters. These modes will be then arranged on the timeline consequently. Based on the identified modes and pointing budget, the architecture of the actual system will be presented and then progressively analyzed, verifying the compliance with the previously found requirements. Finally, a reverse sizing of AOCS will be carried out.

## 4.2 Breakdown of Juno modes

Throughout the mission phases, Juno has to accomplish different tasks through various modes. The principal ones that have been identified are here described.

### 4.2.1 Sun Pointing Mode (SPM)

This mode aims at pointing the spin axis of S/C (+Z axis) to the Sun. This mode is used in order to:

- keep the solar panels pointed to the Sun to provide energy; this is even more crucial in the initial phases of the mission, when all the system checkouts have to be performed;
- thermally protect the satellite's vault using the HGA as a shield when the satellite is relatively close to the Sun.

This mode is applied mainly when the SPE angle is too large to ensure the communication through the HGA. This condition occurs when the satellite is in proximity of Earth and relatively near to the Sun during the interplanetary phase. The LGAs are therefore used during this mode to communicate with ground.
The pointing requirement for this mode is not very strict since the solar panels are sized for much higher distances and can provide enough energy, the LGAs have a wide beamwidth to communicate with ground and the HGA is large enough to protect the vault.

### 4.2.2 Earth Pointing Mode (EPM)

### 4.2.3 GRAVity science Mode (GRAVM)

### 4.2.4 MicroWave Radiometer Mode (MWRM)

### 4.2.5 Turn-Burn-Turn Mode (TBTM)

### 4.2.6 VECtor Mode (VECM)

### 4.2.7 Spin Change Mode (SCM)

### 4.2.8 Safe Modes

## 4.3 Architecture and rationale of AOCS

## 4.4 Reverse sizing of AOCS

# Bibliography

[1]  Richard Grammier. *Overview of the Juno Mission to Jupiter*. Site: `https://www.jpl.nasa.gov/missions/juno`. 2006.